ADBA Computer Science
Cutting-Edge Scientific Solutions

e-ISSN: 3023-8544
RESEARCH ARTICLE
Vol.3 / No.1 / 2026 / pp.37-50
https://doi.org/10.69882/adba.cs.2026016

Stochastic Weather Simulation of Türkiye's Geographical Regions: A Monte Carlo Framework

Nihan Hüsna Kılıç[*,1] **and Abdullah Sevin**[α,2]

[*]Institute of Science, Data Science and Artificial Intelligence Program, Sakarya University, Sakarya, Türkiye, [α]Faculty of Computer and Information Sciences, Computer Engineering, Sakarya University, Sakarya, Türkiye.

ABSTRACT Understanding and predicting regional climatic variations is crucial for agricultural planning, water resource management, and disaster mitigation in the face of increasing global climate instability. This study presents a comprehensive stochastic simulation framework designed to model the diverse meteorological profiles of Türkiye's seven geographical regions. The developed model utilizes a randomized structure that learns monthly parameters from historical daily datasets spanning the 2010–2024 period and generates daily temperature and precipitation scenarios for 2025. Methodologically, a Normal Distribution was employed for temperature modeling, while a first-order Markov Chain was utilized to determine the occurrence of precipitation. To account for the characteristically positive and right-skewed nature of rainfall intensity on wet days, the Gamma Distribution was preferred a standard approach in current literature for modeling daily precipitation amounts. To capture the inherent stochasticity of atmospheric processes, a Monte Carlo simulation approach was implemented. Each representative city was initially simulated with 300 iterations to ensure statistical robustness. To rigorously assess predictive accuracy, validation for 2024 was performed using a Monte Carlo simulation with 400 independent runs. The findings demonstrate that the model effectively captures regional climatic trends and provides a reliable synthetic dataset for environmental planning. Validation metrics indicate strong agreement between modeled and observed climatic behavior, with historical monthly temperatures, precipitation totals, and wet-day probabilities consistently falling within the simulated 95% confidence intervals. These results suggest that integrated stochastic models offer a high-fidelity and computationally efficient alternative to complex numerical weather predictors for regional climate assessment.

KEYWORDS
Monte carlo simulation
Stochastic weather modeling
Precipitation simulation
Temperature modeling
Markov chain

INTRODUCTION

The accurate representation and prediction of climatic variables are fundamental components of environmental modeling, influencing critical sectors such as agriculture, energy management, and urban planning. Due to the complex and chaotic nature of the atmosphere, traditional deterministic approaches often fall short of capturing the full spectrum of climatic variability. In this context, modeling and simulation approaches leverage statistical behaviors learned from historical data to generate probabilistic forecasts (Palmer *et al.* 2005).

When historical weather patterns are examined, it is observed that even under identical initial conditions, varying outcomes can emerge due to inherent atmospheric uncertainty. Therefore, relying on a single deterministic forecast is insufficient for realistic modeling (Palmer 2000). To address this, multiple potential scenarios must be simulated to measure precision and quantify uncertainty. This study aims to stochastically model the temperature and precipitation processes of seven representative cities from Türkiye's diverse climatic regions. The results are reported in terms of monthly mean temperature, the probability of precipitation, and mean total precipitation with a 95% confidence interval, aiming to achieve high-fidelity estimations. To interpret atmospheric uncertainty, the Monte Carlo simulation method was employed, allowing the same model to be executed numerous times to observe the distribution of results. To ensure stable confidence intervals while maintaining computational efficiency, 300 iterations were performed for each city.

In research focusing on stochastic weather generation, various statistical approaches are utilized to represent the random nature and temporal continuity of meteorological variables on a daily scale. Within this framework, the occurrence of precipitation is predominantly modeled using Markov chains, while the intensity of rainfall on wet days is characterized by the Gamma distribution which is widely preferred in modeling daily rainfall amounts. This methodology serves as a fundamental building block for widely recognized models such as WGEN and LARS-WG (Semenov *et al.* 1998; Wilks 1999b,a). For continuous variables like temperature and solar radiation, methods based on the Normal distribution assumption are generally preferred. Studies by Wilks have demonstrated that Monte Carlo-based simulations provide an effective framework for producing these variables in a consistent and integrated manner (Wilks 1998). Subsequent research has further investigated the extent to which these stochastic models

Manuscript received: 12 September 2025,
Revised: 18 December 2025,
Accepted: 20 December 2025.

[1]nihanhusnakilic@gmail.com
[2]asevin@sakarya.edu.tr (**Corresponding author**)

reflect both climate variability and extreme precipitation events across different scales. Collectively, Markov chain and probability distribution-based Monte Carlo approaches are considered established and reliable methods in the literature for generating realistic daily weather data.

The development and application of stochastic weather generators (SWGs) have been extensively documented in the literature as effective tools for bridging the gap between coarse climate data and local-scale applications. (Schuol and Abbaspour 2007) emphasized the utility of using monthly weather statistics to generate daily data, demonstrating that such approaches can provide robust inputs for hydrological models like SWAT (Soil and Water Assessment Tool). Similarly, (Kilsby *et al.* 2007)] highlighted the importance of daily weather generators in climate change studies, providing a framework. Recent advancements in the field have shifted towards more sophisticated probabilistic structures.

(Ailliot *et al.* 2015) provided a comprehensive overview of weather-type models, categorizing the evolution of SWGs and their ability to capture different atmospheric states. More recently, (Guan *et al.* 2025) evaluated the performance of regional stochastic generators, specifically focusing on their ability to reproduce heavy-precipitation events across various spatial and temporal scales. Their findings reinforce the reliability of stochastic approaches in representing extreme meteorological phenomena, a critical requirement for modern hazard and risk assessments. In parallel, recent studies have expanded stochastic weather generator capabilities by improving precipitation representation, uncertainty characterization, applicability to climate-risk assessments and simulation of extreme weather events (Najibi *et al.* 2024; Woodson *et al.* 2025; Nandan *et al.* 2024; Semenov 2008). This body of research provides a solid foundation for the methodology adopted in this study, which integrates established Markovian and distributional techniques to model the regional climate variability of Türkiye.

For this study, daily temperature and precipitation data were retrieved via the Open-Meteo Archive API (Zippenfenig 2023). Using the specific latitude and longitude coordinates for each city, daily mean temperature and total precipitation values were downloaded for the period between January 1, 2010, and December 31, 2024. Seven cities were selected to represent all geographical regions of Türkiye, enabling a comparative analysis of different climate types within a unified modeling framework. Daily observation data for the 2010–2024 period were retrieved for all representative cities to serve as the foundation for parameter estimation and simulation. To ensure physical consistency and exclude stochastic noise from trace amounts (e.g., light drizzle), a daily precipitation threshold of 1.0 mm was established.

To ensure that the stochastic projections are both robust and scientifically defensible, the modeling process is structured into two distinct stages: Validation and Future Scenario Generation. In the first stage, the model's performance is evaluated against independent historical observations from the year 2024, which were withheld during the initial parameter fitting phase. This assessment confirms the framework's ability to accurately reproduce regional climatic statistics. Following successful validation, stochastic simulations are then conducted for the future year of 2025. This dual-stage approach ensures that the projected scenarios are grounded in demonstrated statistical performance rather than simple extrapolation, providing a more reliable basis for regional climate assessment.

METHODOLOGY

Stochastic Framework and Simulation Logic

Atmospheric processes are inherently stochastic, and a single simulation output is insufficient to represent the full spectrum of possible climatic behaviors. Consequently, Monte Carlo-based approaches are widely employed in weather generation literature. (Wilks 1999a) demonstrated that multiple simulations are critical for uncertainty analysis in the simultaneous generation of variables such as daily temperature and precipitation. Similarly, (Knutti *et al.* 2008) emphasized that confidence intervals in climate projections can only be meaningfully interpreted through multi-scenario ensembles. In this study, temperature was modeled using a monthly Normal Distribution, precipitation occurrence via a first-order Markov Chain, and precipitation intensity—conditional on a wet day—via a Gamma Distribution. The modeling framework is based on the following assumptions:

- Daily temperature acts as a continuous random variable with a nearly symmetric distribution.
- Precipitation occurrence exhibits temporal dependency between successive days.
- Precipitation intensity is a continuous, non-negative, and right-skewed variable.

Mathematical Modeling of Variables

Monthly mean and standard deviation values were used to sample daily temperatures from a Normal Distribution. For precipitation, since wet and dry states are not statistically independent, a first-order Markov Chain was utilized. Because wet and dry days tend to cluster in time, precipitation occurrence is commonly modeled with a two-state, first-order Markov chain, where the probability of a wet day depends on the previous day's state (Wilks 1999b,a). The process is defined as a binary state (W=1 for wet, W=0 for dry), and transition probabilities were calculated. Monthly transition probabilities were estimated directly from observed wet/dry sequences using empirical frequencies. A "wet day" was defined as having a total daily precipitation at least 1.0 mm. This threshold was selected to exclude trace events such as drizzle, which would otherwise alter the probability distribution and diminish the model's realism.

Since daily precipitation amounts are strictly positive and exhibit pronounced right-skewness, the Gamma Distribution was employed to represent asymmetric rainfall behavior. During model development, alternative formulations such as the Generalized Extreme Value (GEV) for extreme event analysis or Skew-Normal distributions for asymmetric temperature behavior were considered. However, as the primary objective of this study is to represent regional climatic variability at a monthly scale rather than focusing on rare extremes, the Gamma and Normal distributions were deemed sufficient and computationally efficient, in line with recent literature (Najibi *et al.* 2024; Woodson *et al.* 2025; Nandan *et al.* 2024).

The simulation framework follows a two-phase process: (1) Parameter Learning, where historical data are used to estimate transition probabilities and distribution parameters, and (2) Stochastic Generation, where daily variables are synthesized based on the learned states. To ensure statistical stability, the year 2025 was simulated using a 400-run Monte Carlo ensemble for each city. All simulations utilized a fixed random seed to ensure reproducibility, with calendar structures (month lengths) corresponding to the year 2024.

The year 2025 was simulated using a 300-run Monte Carlo ensemble for each city to characterize potential future variability. In the current implementation, month lengths were based on the 2024 calendar structure; this choice defines the temporal framework and does not affect the learned stochastic parameters. This ensemble approach aims to stabilize uncertainty intervals and provide a comprehensive distribution of possible outcomes. To ensure reproducibility, all simulations were generated using a fixed random seed (RNG_SEED=42). Furthermore, the model's predictive performance was rigorously tested using an extended 400-run validation ensemble for the year 2024.

Mathematical Framework and Operational Principles

In this study, daily weather processes are modeled using monthly parameters derived from historical observations. The model represents temperature and precipitation through separate yet internally consistent stochastic components.

- Daily Average Temperature Generation:

Daily mean temperature is generated using a Normal distribution based on monthly parameters. For a given month m, the temperature process is defined as 1:

$$T_t \sim N\left(\mu_m, \sigma_m^2\right) \tag{1}$$

where μ_m and σ_m^2 represent the mean temperature and standard deviation for month m, respectively, estimated from observation data between 2010 and 2024. The Normal distribution was selected due to the approximately symmetric distribution of temperature at the monthly scale.

- Precipitation Occurrence (First-Order Markov Chain)

Due to the temporal persistence of wet weather, the state of precipitation is modeled using a first-order Markov Chain. The precipitation state is defined as a binary random variable: $W_t \in \{0, 1\}$ where W_t=1 denotes a wet day and W_t=0 denotes a dry day. The probability of a wet day depends on the state of the previous day shown in 2 and 3:

$$P\left(W_t = 1 \mid W_{t-1} = 1\right) = p_{11,m} \tag{2}$$

$$P\left(W_t = 1 \mid W_{t-1} = 0\right) = p_{01,m} \tag{3}$$

Here, $p_{11,m}$ and $p_{01,m}$ represent the conditional transition probabilities for month m. These probabilities were estimated directly from empirical wet/dry transition frequencies within the historical record. In instances or specific months where precipitation events are extremely rare, transition probabilities may approach boundary values (0 or 1). This behavior is maintained within the model as it accurately reflects the observed scarcity of meteorological transitions in the specific regional climate history, ensuring that the synthetic series remains grounded in empirical reality.

- Daily Precipitation Amount

The daily total precipitation amount is modeled conditionally upon the occurrence of a wet day. For a day t where W_t=1, the amount P_t follows a Gamma distribution as 4:

$$P_t \mid \left(W_t = 1\right) \sim \Gamma\left(k_m, \theta_m\right) \tag{4}$$

If $W_t = 0$, then P_t=0. The Gamma distribution was chosen to represent the characteristic right-skewed nature of rainfall intensity, where values are strictly positive and extreme amounts occur with low frequency. Since daily precipitation amounts are strictly positive and exhibit pronounced right-skewness, particularly due to intermittent heavy rainfall events, the Gamma distribution was employed to represent rainfall intensity on wet days. Although alternative distributions (e.g., mixed exponential or extreme value formulations) may outperform the Gamma distribution in specific settings, Gamma remains a common and practical choice in stochastic weather generators, particularly when the focus is on monthly-scale variability rather than extremes (Semenov *et al.* 1998; Wilks 1999b). The shape parameter (k_m) and scale parameter (θ_m) were estimated from wet-day observations within the corresponding month.

- Uncertainty Evaluation (Monte Carlo Simulation)

To evaluate uncertainty, the model was iterated 300 times for each representative city. All realizations were generated as stochastic draws from a single seeded random-number generator stream, ensuring reproducibility while yielding distinct ensemble members. The 95% confidence intervals for monthly metrics were calculated using the quantiles of the resulting Monte Carlo sample distributions in 5:

$$CI_{95\%} = \left[Q_{0.025}, Q_{0.975}\right] \tag{5}$$

This approach allows for a quantitative assessment of not only the average behavior but also the inherent variability and uncertainty in the synthetic weather data. Recent studies highlight that ensemble-based confidence bands provide an interpretable way to communicate uncertainty in climate-sensitive applications (Woodson *et al.* 2025; Nandan *et al.* 2024). For the 2025 simulation experiments, 300 Monte Carlo realizations were employed. This ensemble size was selected to balance statistical stability in monthly means and 95% confidence intervals with computational efficiency. Overall, the literature indicates that Markov-chain-based occurrence models combined with parametric distributions—such as the Gamma and Normal distributions used in this study—can effectively reproduce realistic mean behavior and variability at daily to monthly scales (Ailliot *et al.* 2015).

RESULTS AND DISCUSSION

Stochastic weather generators based on Markov chains and parametric probability distributions have been proven to realistically reproduce both mean climate behavior and variability at daily and monthly scales (Ailliot *et al.* 2015). Furthermore, recent studies highlight that Monte Carlo ensembles and probabilistic summaries significantly improve interpretability when comparing simulated outcomes against observed climate indicators (Najibi *et al.* 2024; Woodson *et al.* 2025; Nandan *et al.* 2024). Building on this established framework, this section presents the outputs of the stochastic weather simulation for the year 2025 across seven representative cities of Türkiye.

The findings are categorized into monthly temperature trends, precipitation occurrences, and total rainfall intensity. By utilizing the 300-run Monte Carlo ensemble, the results provide not only the expected mean values but also the probabilistic boundaries of potential climatic shifts. The following sub-sections evaluate the model's performance in capturing regional climatic characteristics ranging from the humid subtropical profile of the Black Sea to the semi-arid conditions of Central and Southeastern Anatolia through comparative tables and visual distribution plots.

The temperature trends, as shown in Figure 1, indicate that the lowest mean temperatures occur during January and February. A steady upward trend is observed during the summer months, followed by a gradual cooling phase starting from autumn. Similar to the precipitation patterns, the 95% confidence interval for temperature is broader in the winter and more constrained in the summer. This finding suggests that winter temperatures are subject to greater stochastic variability, while summer heatwaves or average temperatures follow a more predictable trajectory. These results are in full alignment with the transitional climate characteristics of the Marmara Region.

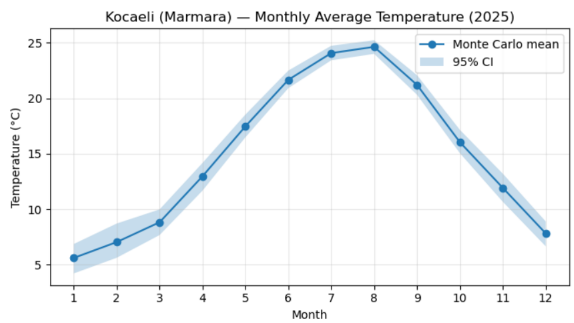

Figure 1 Monthly Average Temperature of Kocaeli

The simulation results for the Marmara region, represented by Kocaeli, demonstrate high seasonal consistency with historical climatic patterns. As illustrated in Figure 2, the probability of precipitation reaches its peak during the winter months and significantly declines throughout the summer period. The 95% confidence interval is notably wider during the winter, suggesting that precipitation events in this season exhibit higher irregularity and variance. Conversely, the narrow confidence interval observed in the summer months indicates that dry conditions are more stable and frequent during this period.

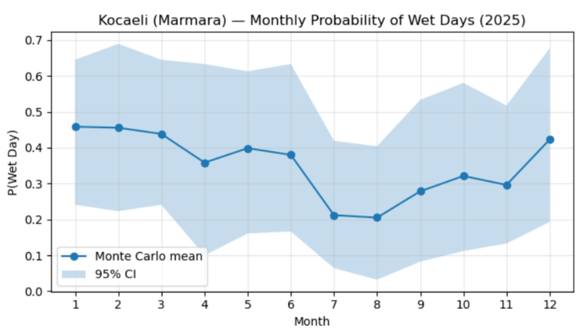

Figure 2 Monthly Probability of Wet Days of Kocaeli

Furthermore, the monthly precipitation intensity values presented in Table 1 confirm that the highest total rainfall amounts are concentrated in the autumn and winter seasons. The significant decrease in total precipitation during the summer months highlights the model's ability to accurately reflect the regional dry season.

Regarding temperature trends shown in Figure 3, the simulation results are highly consistent with the regional climate. The 95% confidence interval for temperature remains remarkably stable and narrow throughout the year, indicating low inter-annual temperature variability for this province. This suggests that daily mean temperatures in Izmir follow a more predictable seasonal trajectory compared to other regions.

The simulation results for Izmir, as the representative city of the Aegean Region, accurately reflect the transition between seasons. As illustrated in Figure 4, the probability of precipitation decreases

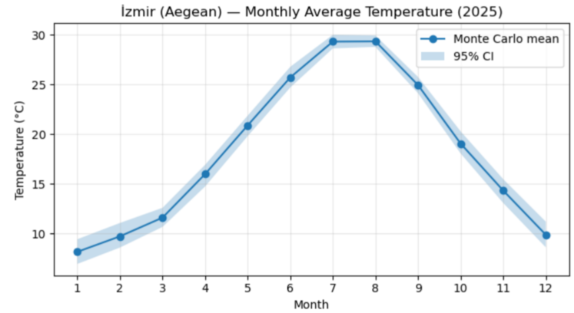

Figure 3 Monthly Average Temperature of Izmir

gradually from winter to spring, shows a slight increase during the mid-spring period, and reaches its minimum during the summer months before trending upward in autumn. Notably, the precipitation probability in July and August is near zero, suggesting that these months may remain entirely dry under typical conditions.

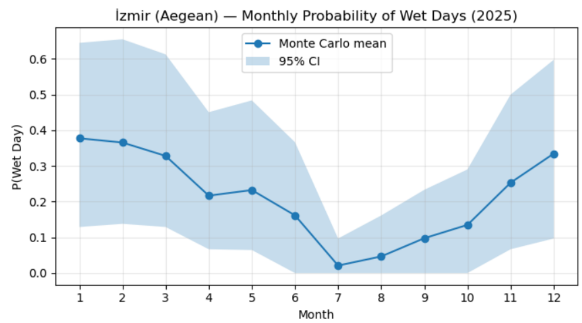

Figure 4 Monthly Probability of Wet Days of Izmir

A comparative analysis of monthly total precipitation and the probability of wet days (Table 2) reveals a high degree of correlation. However, the widening of confidence intervals specifically during the winter months indicates that uncertainty in precipitation intensity is significantly higher than that of temperature. Overall, the stochastic outputs for Izmir are in full agreement with the characteristic Mediterranean-influenced Aegean climate, capturing both the summer aridity and the variability of winter rainfall.

The simulation results for Antalya, as shown in Figure 5, are in high alignment with the classical Mediterranean climate profile. In months where the 95% confidence interval is narrow, a stable thermal regime prevails. Conversely, in months where the interval relatively widens, it can be inferred that meteorological uncertainty and inter-annual variability are higher. Overall, the model successfully captures the "hot-summer Mediterranean" (Csa) characteristics, particularly highlighting the high variance in winter precipitation against the predictable aridity of the summer.

As illustrated in Figure 6, the probability of wet days in Antalya significantly increases during the winter months while exhibiting a sharp decline during the summer. The narrow confidence intervals observed during the summer months indicate that the absence of precipitation is statistically stable and consistent during this period. An analysis of monthly total precipitation amounts (Table 3) reveals that rainfall is concentrated in the winter season, both in terms of frequency and intensity.

The simulation results presented in Figure 7 are highly consistent with the typical continental climate of Central Anatolia,

Table 1 Monthly statistical summary of simulated temperature and precipitation parameters of Kocaeli

Month	T_{mean}	T_{low}	T_{high}	W_{prob}	W_{low}	W_{high}	P_{mean}	P_{low}	P_{high}
01	5.61	4.21	6.86	0.46	0.24	0.65	96.24	37.27	162.59
02	7.04	5.62	8.71	0.46	0.22	0.69	84.35	29.15	153.88
03	8.83	7.67	9.98	0.44	0.24	0.65	83.75	39.21	150.66
04	12.97	11.67	14.17	0.36	0.10	0.63	67.47	16.34	130.52
05	17.47	16.48	18.53	0.40	0.16	0.61	74.33	24.58	132.77
06	21.66	20.91	22.49	0.38	0.17	0.63	79.54	18.33	149.30
07	24.07	23.42	24.73	0.21	0.06	0.42	37.36	3.35	97.18
08	24.63	24.01	25.23	0.21	0.03	0.40	33.17	0.70	89.40
09	21.20	20.32	22.08	0.28	0.08	0.53	54.12	5.52	119.56
10	16.04	15.05	17.15	0.32	0.11	0.58	84.55	15.07	191.06
11	11.92	10.67	13.20	0.30	0.13	0.52	69.32	17.75	136.07
12	7.82	6.66	8.90	0.42	0.19	0.68	100.94	34.84	181.49

Table 2 Monthly statistical summary of simulated temperature and precipitation parameters of Izmir

Month	T_{mean}	T_{low}	T_{high}	W_{prob}	W_{low}	W_{high}	P_{mean}	P_{low}	P_{high}
01	8.18	6.97	9.44	0.38	0.13	0.65	130.35	29.17	251.79
02	9.73	8.61	11.08	0.37	0.14	0.66	95.37	22.50	192.31
03	11.62	10.69	12.60	0.33	0.13	0.61	79.79	12.71	167.38
04	15.99	14.75	16.92	0.22	0.07	0.45	54.53	4.96	129.37
05	20.89	19.81	21.86	0.23	0.06	0.48	45.69	6.79	107.60
06	25.70	24.69	26.77	0.16	0.00	0.37	27.47	0.00	71.77
07	29.30	28.62	29.99	0.02	0.00	0.10	2.00	0.00	10.66
08	29.32	28.77	29.91	0.05	0.00	0.16	3.98	0.00	15.49
09	24.93	24.11	25.74	0.10	0.00	0.23	18.13	0.00	62.27
10	19.06	18.06	20.28	0.13	0.00	0.29	55.01	0.00	169.76
11	14.34	13.09	15.48	0.25	0.07	0.50	80.87	10.02	192.93
12	9.89	8.63	11.21	0.33	0.10	0.60	111.20	16.15	240.03

characterized by hot, arid summers and cold, unstable winters. The model accurately captures the seasonal fluctuations in both temperature and rainfall, providing a realistic representation of the region's atmospheric dynamics.

As illustrated in Figure 8, the probability of wet days in Ankara is notably higher during the spring months compared to the summer, with a further increasing trend observed throughout the autumn. The widening of the confidence intervals during these transitional periods suggests that the precipitation regime (Table 4) in Ankara exhibits significant variability during seasonal shifts.

According to the temperature trends shown in Figure 9, the relatively narrow confidence intervals indicate a stable thermal regime. The data suggests that Trabzon experiences a temperate climate where extreme temperature fluctuations are mitigated. This stability reflects the moderating influence of the sea, which prevents drastic seasonal shifts and maintains a consistent temperature trajectory as captured by the simulation model.

As illustrated in Figure 10, the probability of wet days in Trabzon remains high throughout the year, with this trend persisting even during the summer months. This result is highly consistent with the characteristic year-round precipitation regime of the Black Sea region.

The breadth of the confidence intervals across the simulated period suggests that while rainfall is frequent, its daily intensity and occurrence exhibit significant stochastic variability in the representative city. The comprehensive statistical breakdown of these

Table 3 Monthly statistical summary of simulated temperature and precipitation parameters of Antalya

Month	T_{mean}	T_{low}	T_{high}	W_{prob}	W_{low}	W_{high}	P_{mean}	P_{low}	P_{high}
01	9.43	8.55	10.33	0.42	0.19	0.68	242.21	74.93	465.64
02	10.43	9.54	11.26	0.36	0.14	0.66	135.95	23.24	300.43
03	12.39	11.59	13.16	0.29	0.10	0.52	96.88	15.63	220.63
04	16.05	15.22	16.87	0.23	0.07	0.43	54.21	7.56	120.09
05	20.38	19.51	21.26	0.24	0.03	0.45	59.66	3.80	165.13
06	25.21	23.97	26.46	0.13	0.00	0.30	17.72	0.00	49.94
07	29.45	28.76	30.21	0.04	0.00	0.16	5.13	0.00	30.62
08	29.26	28.69	29.96	0.05	0.00	0.16	5.44	0.00	22.72
09	25.81	25.07	26.58	0.08	0.00	0.23	22.58	0.00	85.50
10	20.31	19.50	21.21	0.19	0.03	0.39	105.56	0.51	277.51
11	15.25	14.48	15.98	0.24	0.03	0.50	103.83	1.59	254.29
12	11.12	10.17	11.95	0.40	0.14	0.68	207.76	41.94	418.76

Table 4 Monthly statistical summary of simulated temperature and precipitation parameters of Ankara

Month	T_{mean}	T_{low}	T_{high}	W_{prob}	W_{low}	W_{high}	P_{mean}	P_{low}	P_{high}
01	1.11	-0.64	2.80	0.32	0.13	0.52	56.52	18.71	110.80
02	3.50	1.86	5.12	0.28	0.07	0.55	39.61	4.64	82.09
03	6.37	4.96	7.85	0.33	0.11	0.58	55.79	14.02	108.68
04	11.91	10.53	13.26	0.29	0.08	0.50	35.99	6.37	72.16
05	16.49	15.14	17.53	0.34	0.14	0.60	53.81	16.59	108.31
06	20.52	19.56	21.56	0.30	0.07	0.57	43.97	5.43	88.99
07	24.49	23.57	25.35	0.06	0.00	0.16	6.42	0.00	22.83
08	25.00	24.18	25.86	0.08	0.00	0.23	7.62	0.00	24.84
09	20.61	19.42	21.93	0.07	0.00	0.20	12.66	0.00	61.68
10	13.97	12.63	15.27	0.15	0.00	0.37	25.83	0.00	65.45
11	8.05	6.81	9.36	0.16	0.00	0.37	33.38	0.00	84.86
12	3.38	2.18	4.49	0.28	0.06	0.52	49.36	6.94	106.79

parameters is provided in Table 5.

As illustrated in Figure 11 and Figure 12, the simulation results for Erzurum are highly consistent with the severe continental climate of Eastern Anatolia. During the winter months, mean temperatures remain significantly below freezing (negative Celsius values). The relatively wide confidence intervals observed in this period suggest that the region is subject to extreme cold spells and high thermal variability.

Regarding precipitation patterns in Table 6, the probability of wet days reaches its peak during the spring months and exhibits a notable decline during the summer season. These findings reflect the regional characteristics where snowmelt and spring convective rains are dominant, followed by a relatively drier but short summer period. The model accurately captures the harsh seasonal transitions and the rigorous winter conditions unique to the high-altitude geography of Erzurum.

As illustrated in Figure 13, the simulated mean temperatures for Diyarbakır exceed 30°C during the summer months and fall below 5°C during the winter. The prevalence of a narrow confidence interval suggests that these high temperatures are observed with significant stability and predictable seasonal intensity. Furthermore, the results in Figure 14 indicate that the probability of a wet day is nearly zero during the summer season, while it shows a marked increase during the winter months. These findings and also Table 7 are in full alignment with the semi-arid climatic characteristics of Southeastern Anatolia, specifically reflecting the intense

Table 5 Monthly statistical summary of simulated temperature and precipitation parameters of Trabzon

Month	T_{mean}	T_{low}	T_{high}	W_{prob}	W_{low}	W_{high}	P_{mean}	P_{low}	P_{high}
01	6.61	5.33	7.83	0.43	0.19	0.69	102.77	36.61	176.18
02	7.45	6.20	8.76	0.45	0.24	0.69	78.88	32.24	128.78
03	8.76	7.30	10.07	0.52	0.32	0.73	114.02	50.38	185.65
04	12.65	11.39	13.95	0.46	0.20	0.70	105.48	36.01	185.68
05	16.56	15.54	17.64	0.51	0.27	0.74	131.67	56.32	219.43
06	20.67	19.86	21.26	0.54	0.27	0.80	117.93	51.86	200.87
07	22.77	22.23	23.37	0.52	0.29	0.74	106.25	41.71	193.97
08	23.54	23.01	24.03	0.56	0.29	0.81	117.68	34.08	238.98
09	20.71	19.88	21.50	0.54	0.28	0.77	155.39	65.74	268.90
10	16.41	15.39	17.33	0.51	0.26	0.74	180.33	70.63	305.10
11	12.36	11.19	13.62	0.38	0.13	0.65	107.86	27.00	199.07
12	8.84	7.51	10.04	0.35	0.16	0.61	84.85	26.09	172.29

Table 6 Monthly statistical summary of simulated temperature and precipitation parameters of Erzurum

Month	T_{mean}	T_{low}	T_{high}	W_{prob}	W_{low}	W_{high}	P_{mean}	P_{low}	P_{high}
01	-5.86	-7.31	-4.45	0.29	0.10	0.50	42.58	9.73	81.93
02	-4.32	-5.67	-2.92	0.28	0.07	0.52	34.92	7.61	70.73
03	-0.33	-1.64	0.85	0.43	0.23	0.65	77.54	33.11	130.13
04	5.47	4.29	6.61	0.51	0.30	0.77	81.67	36.19	135.67
05	10.32	9.21	11.21	0.64	0.42	0.84	111.88	62.88	167.46
06	15.55	14.60	16.60	0.40	0.17	0.63	65.33	22.36	118.54
07	18.91	18.07	19.77	0.27	0.10	0.48	43.51	10.02	82.22
08	19.94	18.99	20.75	0.16	0.03	0.32	20.46	2.28	48.01
09	15.61	14.47	16.63	0.17	0.00	0.37	22.07	0.00	53.15
10	8.69	7.58	9.82	0.27	0.06	0.53	39.84	7.36	85.38
11	2.07	0.83	3.27	0.23	0.03	0.53	36.32	1.97	86.45
12	-3.68	-5.22	-2.21	0.23	0.06	0.50	36.79	5.03	87.59

summer aridity and the concentrated winter precipitation regime. The model effectively captures the regional contrast between the extreme heat of the dry season and the relatively mild, wet winter period.

The aggregated simulation results in Table 8 for the seven geographical regions of Türkiye are summarized in the table above, providing a comparative overview of annual average temperatures and the probability of wet days, illustrated in also Figure 15 and Figure 16. The stochastic model demonstrates high sensitivity to regional variations, effectively distinguishing between the maritime, continental, and transitional climates of the country. According to the synthesized data, Antalya (Mediterranean) and Izmir (Aegean) exhibit the highest annual average temperatures, approximately 18.8°C and 18.3°C respectively, reflecting their subtropical characteristics. In stark contrast, Erzurum (Eastern Anatolia) presents the lowest annual mean temperature at 6.9°C, consistent with its high-altitude, severe continental climate. Regarding precipitation, Trabzon (Black Sea) stands out as the most humid region with an annual total of 1397.2 mm and the highest frequency of rainy days (174 days), emphasizing its year-round wet climate. Ankara (Central Anatolia) and Diyarbakır (Southeastern Anatolia) recorded the lowest annual rainfall totals (425.2 mm and 594.4 mm respectively), highlighting the semi-arid nature of the inland steppes. The consistency in the number of rainy days across 300 iterations (ranging from 78 to 174 days depending on the region) validates the robustness of the 1st-order Markov Chain and the 1.0 mm wet threshold

Table 7 Monthly statistical summary of simulated temperature and precipitation parameters of Diyarbakır

Month	T_{mean}	T_{low}	T_{high}	W_{prob}	W_{low}	W_{high}	P_{mean}	P_{low}	P_{high}
01	3.21	2.16	4.20	0.38	0.10	0.65	94.45	24.63	183.92
02	5.04	3.86	6.33	0.35	0.14	0.62	72.44	21.38	145.61
03	8.79	7.72	9.95	0.44	0.18	0.65	106.55	26.81	202.81
04	14.27	13.26	15.34	0.35	0.10	0.63	74.84	14.81	155.50
05	19.25	18.04	20.41	0.31	0.10	0.53	57.25	12.18	118.40
06	26.58	25.48	27.55	0.06	0.00	0.17	4.08	0.00	12.86
07	31.36	30.74	32.11	0.00	0.00	0.03	0.00	0.00	0.00
08	31.34	30.77	31.89	0.00	0.00	0.03	0.00	0.00	0.00
09	26.16	25.30	27.11	0.03	0.00	0.15	4.38	0.00	30.35
10	18.33	17.21	19.39	0.15	0.00	0.35	38.82	0.00	111.38
11	10.25	9.11	11.41	0.21	0.03	0.47	54.73	7.28	135.75
12	4.97	3.91	6.03	0.31	0.06	0.57	79.04	16.78	164.34

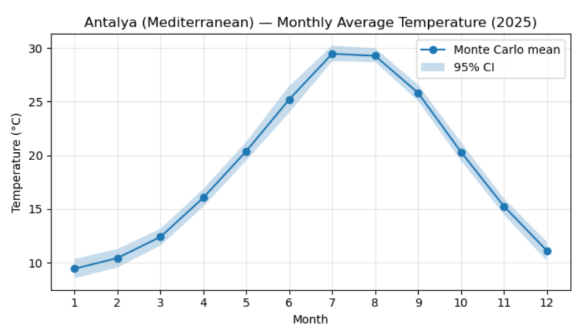

Figure 5 Monthly Average Temperature of Antalya

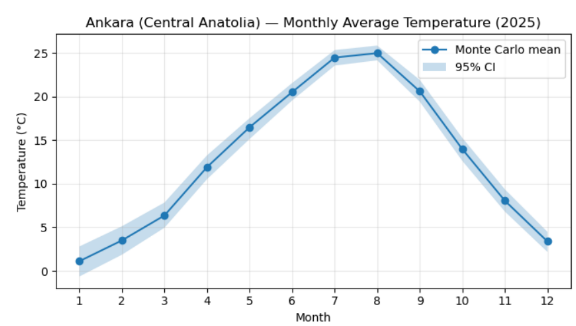

Figure 7 Monthly Average Temperature of Ankara

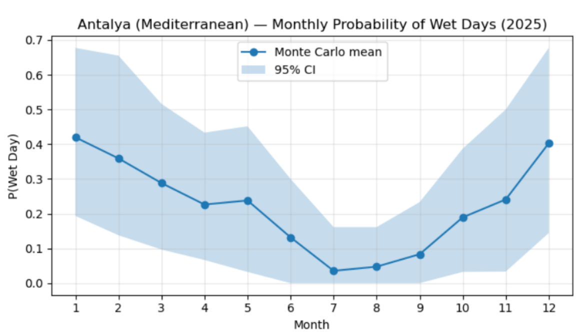

Figure 6 Monthly Probability of Wet Days of Antalya

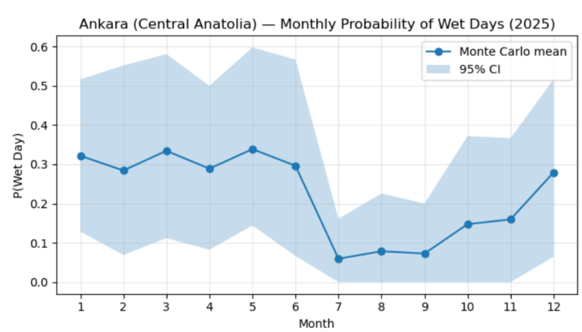

Figure 8 Monthly Probability of Wet Days of Ankara

used in the study. These annual summaries confirm that the integrated stochastic framework can successfully replicate complex regional meteorological balances within a unified mathematical structure.

VALIDATION RESULTS

Model validation was conducted using observed daily climate records from 2024, which were deliberately excluded from the parameter estimation stage and reserved for a strict out-of-sample evaluation. In order to assess uncertainty in a stable and reproducible manner, the stochastic framework was independently simulated for the validation year using a 400-run Monte Carlo ensemble. Although the input data are daily, validation was performed using monthly aggregated indicators, which provide a clear regional-scale comparison. Specifically, the evaluation focused on monthly average temperature, monthly total precipitation, and wet-day probability (fraction of wet days within each

Table 8 Statistical summary of simulated temperature and precipitation parameters of Regions

Region	City	Avg. Temp (°C)	Total Rain (mm)	Rainy Days	Runs	Threshold
Aegean	Izmir	18.27	704.37	78	300	1.0
Black Sea	Trabzon	14.80	1403.11	176	300	1.0
Central Anatolia	Ankara	12.98	420.96	81	300	1.0
Eastern Anatolia	Erzurum	6.90	612.92	118	300	1.0
Marmara	Kocaeli	14.96	865.14	129	300	1.0
Mediterranean	Antalya	18.78	1056.93	81	300	1.0
Southeastern Anatolia	Diyarbakır	16.66	586.58	79	300	1.0

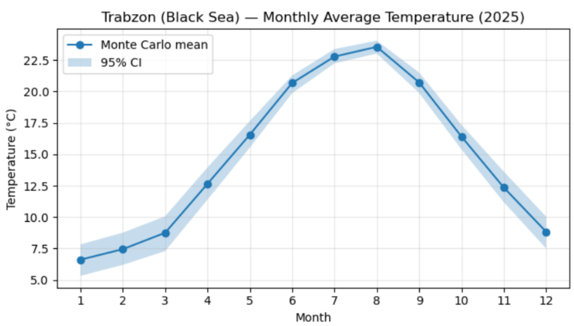

Figure 9 Monthly Average Temperature of Trabzon

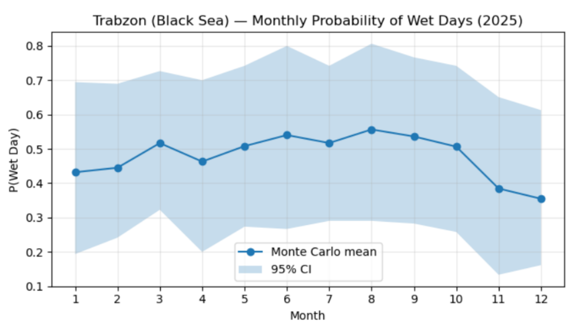

Figure 10 Monthly Probability of Wet Days of Trabzon

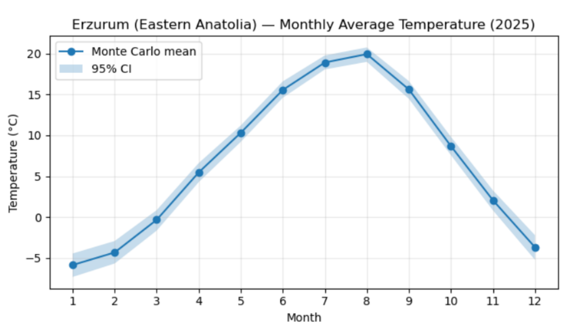

Figure 11 Monthly Average Temperature of Erzurum

month). For each month, the simulation results are summarized using the ensemble mean together with 95% uncertainty bounds derived from the 2.5th and 97.5th percentiles of the Monte Carlo

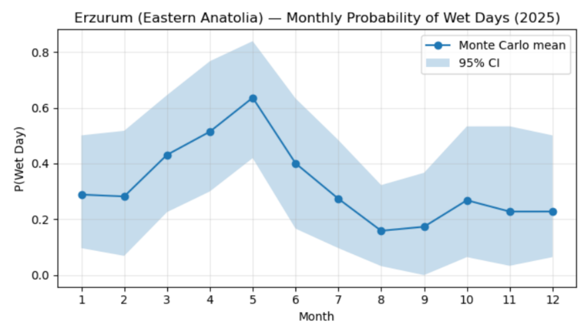

Figure 12 Monthly Probability of Wet Days of Erzurum

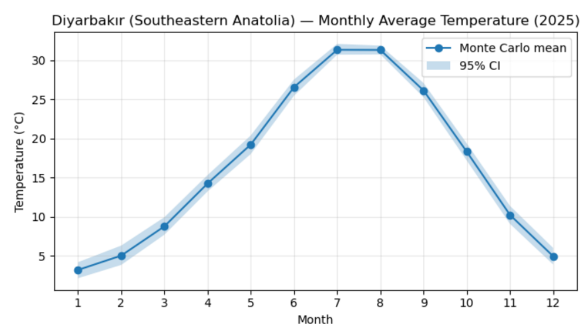

Figure 13 Monthly Average Temperature of Diyarbakır

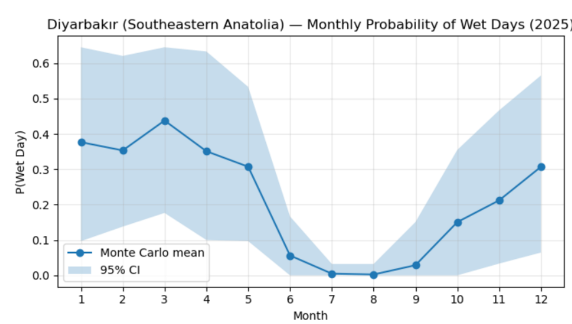

Figure 14 Monthly Probability of Wet Days of Diyarbakır

distribution.

Figure 17 presents the validation results for Kocaeli, representing the Marmara Region. Observed monthly average temperature

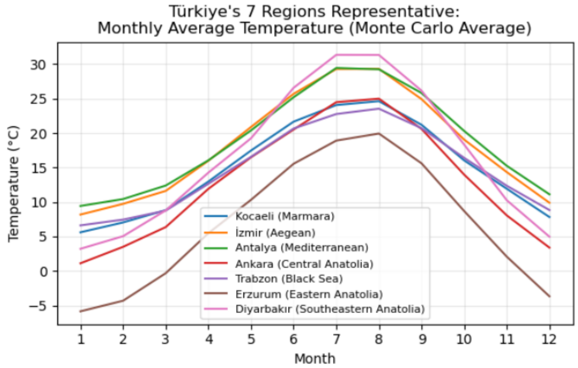

Figure 15 Average Temperature of Regions

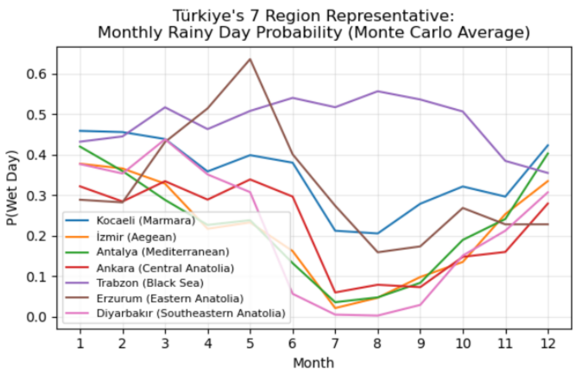

Figure 16 Probability of Wet Days of Regions

values for 2024 closely follow the Monte Carlo ensemble mean and remain within the simulated 95% uncertainty bounds throughout the year. Deviations are generally minor, indicating that the model successfully reproduces the seasonal thermal cycle characteristic of the Marmara climate. Precipitation-related indicators show noticeably wider uncertainty ranges, particularly during winter, reflecting the irregular and event-driven nature of rainfall. Despite this variability, observed monthly total precipitation and wet-day probability remain consistently captured within the ensemble uncertainty bounds. Overall, the results confirm that the combined first-order Markov Chain and Gamma distribution framework provides a reliable representation of both precipitation frequency and intensity for the Marmara Region.

Figure 18 shows validation results for Izmir, representing the Aegean Region. Observed monthly average temperatures align closely with the ensemble mean and remain almost entirely within the 95% uncertainty bounds, which stay relatively narrow across the year. This reflects the strong seasonal predictability of temperature in the Aegean climate. In contrast, precipitation-related variables exhibit broader uncertainty intervals, particularly in winter months, due to higher stochastic variability in rainfall processes. Nevertheless, the model successfully captures the dominant regional pattern, including the pronounced summer dry period. Both observed monthly precipitation totals and wet-day probabilities remain within the simulated uncertainty ranges, confirming that the stochastic framework realistically represents the seasonal precipitation regime typical of the Aegean Region.

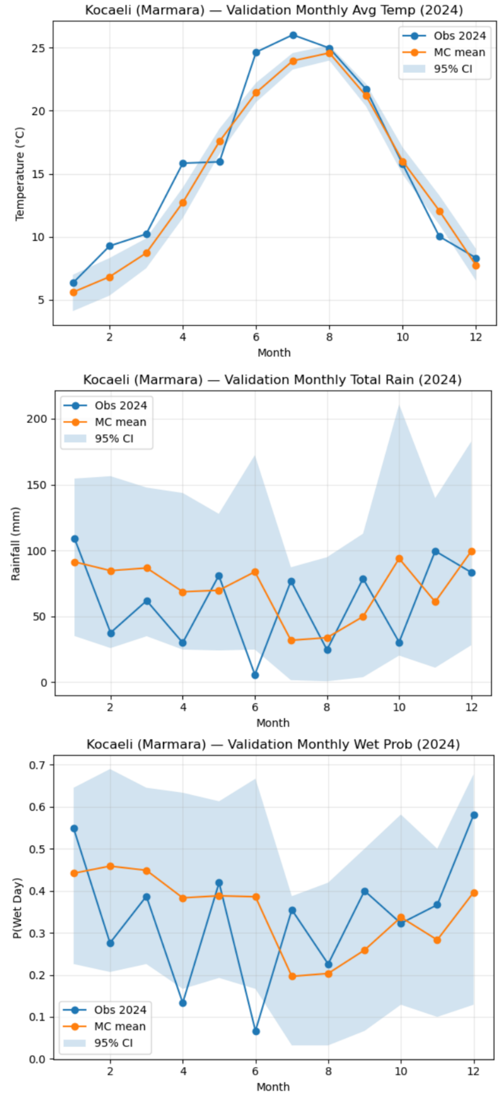

Figure 17 Validation of monthly average temperature, total precipitation, and wet-day probability for Kocaeli (Marmara Region) in 2024

Figure 19 presents the validation results for Antalya, representing the Mediterranean Region. Observed monthly average temperature values closely track the Monte Carlo ensemble mean and consistently fall within the simulated uncertainty bounds. The confidence bands remain particularly narrow during summer, reflecting the stable thermal regime associated with persistent hot-season conditions. Precipitation-related indicators show strong seasonality, with wet-day probability and total precipitation peaking during winter and decreasing sharply during summer. Wider uncertainty bounds during winter indicate increased variability linked to episodic heavy rainfall events, whereas narrow summer uncertainty reflects statistically stable dry conditions. These results demonstrate that the proposed stochastic framework captures the characteristic winter-wet and summer-dry structure of the Mediterranean climate with strong agreement to observations.

Figure 20 illustrates validation results for Ankara, representing the Central Anatolia Region. Observed monthly mean temperatures closely follow the ensemble mean and remain within the 95% uncertainty bounds, indicating that the model accurately reproduces the continental seasonal transition between cold winters

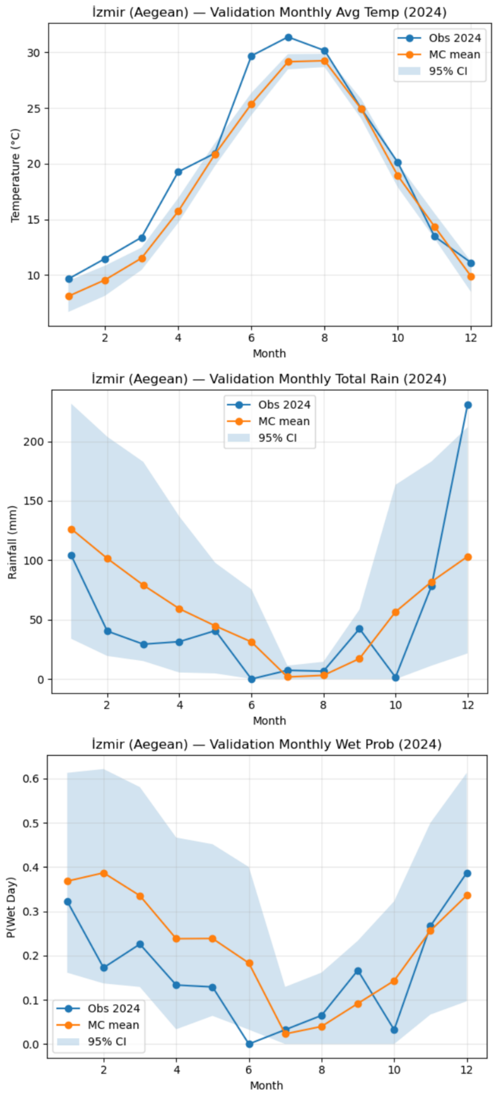

Figure 18 Validation of monthly average temperature, total precipitation, and wet-day probability for Izmir (Aegean Region) in 2024

Figure 19 Validation of monthly average temperature, total precipitation, and wet-day probability for Antalya (Mediterranean Region) in 2024

and warm summers. Precipitation-related indicators exhibit more variability during transitional seasons. Wet-day probability and precipitation totals increase during spring and early summer, followed by a marked decline in mid-summer. The widening of uncertainty bounds during spring suggests increased stochastic variability associated with convective precipitation events, while narrower summer intervals reflect a more stable dry regime. Overall, the results confirm that the framework successfully represents both the thermal cycle and the seasonal timing of precipitation typical of Central Anatolia.

Figure 21 presents validation results for Trabzon, representing the Black Sea Region. Observed monthly mean temperatures remain close to the ensemble mean and stay within the simulated uncertainty bounds, reflecting the relatively moderated thermal variability influenced by the Black Sea. Rainfall-related indicators display consistently high wet-day probabilities across all seasons, including summer months, which is a defining feature of the Black Sea climate. Although uncertainty bounds for precipitation totals and wet-day probability are wider due to variability in rainfall intensity and timing, observed values remain well within the simulated ranges. These findings indicate that the stochastic framework effectively captures the year-round humid precipitation regime characteristic of the Black Sea Region.

Figure 22 shows validation results for Erzurum, representing the Eastern Anatolia Region. Observed monthly average temperatures closely follow the ensemble mean and remain predominantly within the simulated uncertainty bounds. The model successfully reproduces the severe winter conditions, including sustained sub-zero temperatures, reflecting the high-altitude continental climate of Eastern Anatolia. Precipitation-related indicators show pronounced seasonality, with wet-day probability and precipitation totals peaking during spring and decreasing during summer. Wider uncertainty bounds during winter and spring indicate increased variability associated with harsh winter dynamics and seasonal transitions. Despite these challenges, observed values remain within the modeled uncertainty ranges, demonstrating that the framework captures the extreme seasonal contrasts typical of the Eastern Anatolia climate.

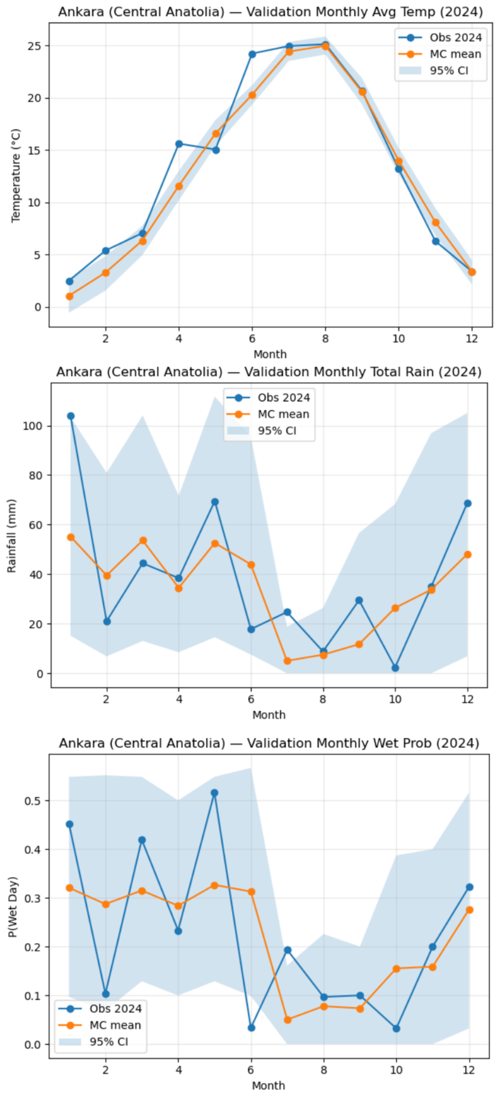

Figure 20 Validation of monthly average temperature, total precipitation, and wet-day probability for Ankara (Central Anatolia Region) in 2024

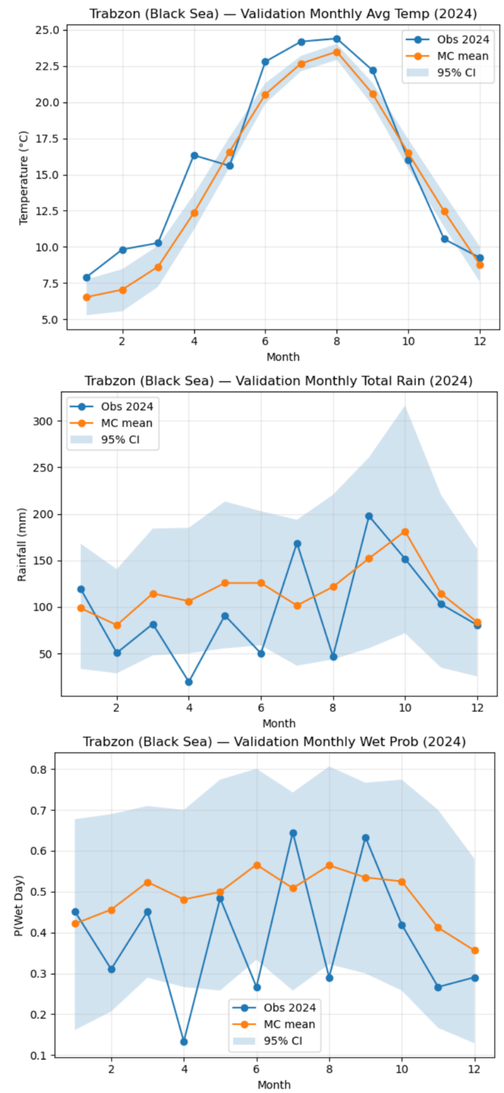

Figure 21 Validation of monthly average temperature, total precipitation, and wet-day probability for Trabzon (Black Sea Region) in 2024

Figure 23 presents validation results for Diyarbakır, representing the semi-arid Southeastern Anatolia Region. Observed monthly mean temperatures closely align with the Monte Carlo ensemble mean and remain within the simulated uncertainty bounds, with particularly stable behavior during the hot summer months. Precipitation-related indicators exhibit a strong seasonal contrast. Wet-day probability and precipitation totals approach near-zero levels during summer, confirming persistent regional aridity, while precipitation occurrence and intensity increase during winter months. Wider uncertainty bounds in winter reflect increased variability linked to episodic rainfall events, whereas narrow summer bounds indicate statistically stable dry conditions. Overall, these results confirm that the stochastic framework successfully captures both the dominant summer dryness and the seasonal concentration of rainfall typical of Southeastern Anatolia.

To complement the visual comparisons between Figures 17 to Figure 23 and Table 9 provides a quantitative summary of model performance across all seven representative regions of Türkiye. The table reports simulated annual mean temperature, total precipitation, and number of wet days for 2025, together with out-of-sample validation errors computed using observed 2024 monthly indicators. Model accuracy is assessed using Mean Absolute Error (MAE) and Root Mean Square Error (RMSE) for monthly average temperature, monthly total precipitation, and wet-day probability. Overall, temperature errors remain consistently low across regions, confirming that the seasonal thermal cycle is reproduced reliably. Precipitation-related errors are comparatively larger, reflecting the inherently intermittent and stochastic nature of rainfall; however, the results remain within acceptable ranges for stochastic weather generator applications. These quantitative findings further support the robustness and generalizability of the proposed stochastic framework across diverse climatic regimes in Türkiye.

Table 9 Annual summary of stochastic simulation results and validation metrics for the seven geographical regions of Türkiye

Region	City	T_{25}	P_{25}	D_{25}	MAE_T	$RMSE_T$	MAE_P	$RMSE_P$	MAE_{Wp}	$RMSE_{Wp}$
Aegean	İzmir	18.27	704.37	78	1.65	2.05	34.70	48.72	0.09	0.11
Black Sea	Trabzon	14.80	1403.11	176	1.66	1.92	42.64	50.00	0.14	0.18
Central Anat.	Ankara	12.98	420.96	81	1.43	1.94	17.33	21.39	0.11	0.14
Eastern Anat.	Erzurum	6.90	612.92	118	1.57	2.02	36.41	46.41	0.09	0.12
Marmara	Kocaeli	14.96	865.14	129	1.54	1.84	34.91	40.40	0.13	0.16
Mediterranean	Antalya	18.78	1056.93	81	1.64	2.10	45.65	54.06	0.13	0.15
S. Eastern Anat.	Diyarbakır	16.66	586.58	79	1.26	1.53	16.93	25.42	0.08	0.11

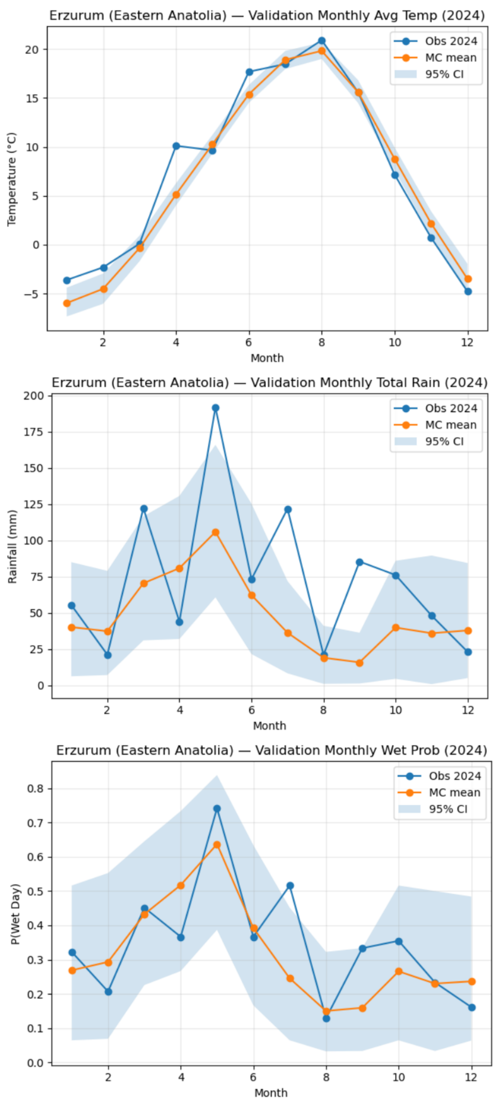

Figure 22 Validation of monthly average temperature, total precipitation, and wet-day probability for Erzurum (Eastern Anatolia Region) in 2024

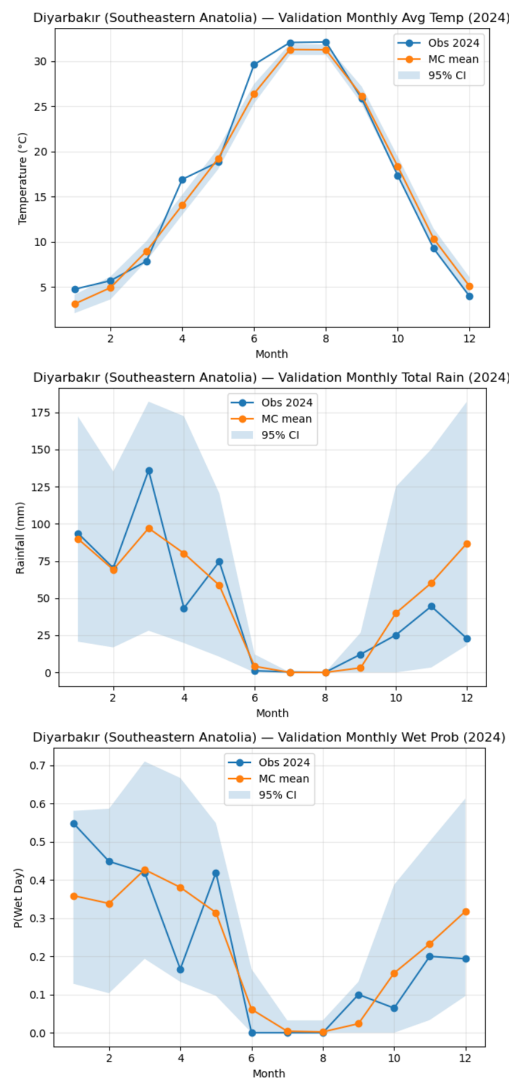

Figure 23 Validation of monthly average temperature, total precipitation, and wet-day probability for Diyarbakır (Southeastern Anatolia Region) in 2024

CONCLUSION

In this study, a Monte Carlo-based stochastic simulation framework was developed and implemented for representative cities across the seven geographical regions of Türkiye. The model successfully synthesized weather data, yielding regionally consistent temperature distributions and precipitation patterns. By leveraging the Monte Carlo approach, atmospheric uncertainty was quantified through probability distributions, allowing for a robust assessment of potential climatic variations.The seasonal behaviors of the 95% confidence intervals align closely with the unique climatic characteristics of each region, confirming that the model provides a reliable representation of regional weather dynamics. Given the inherently stochastic nature of atmospheric processes, this approach captures the natural variability that deterministic models might overlook. Ultimately, the proposed integrated framework offers a computationally efficient and reliable tool for regional climate assessment. The out-of-sample validation using 2024 observations, followed by scenario generation for 2025, further supports the robustness of the model. These findings demonstrate the model's high potential for integration into climate-sensitive decision-support systems, such as agricultural planning, water resource management, and energy infrastructure modeling. Future studies could expand this framework by incorporating non-parametric distributions or multi-site spatial correlations to further refine regional climate risk assessments.

Ethical standard

The authors have no relevant financial or non-financial interests to disclose.

Availability of data and material

The data that support the findings of this study are available from the corresponding author upon reasonable request.

Conflicts of interest

The authors declare that there is no conflict of interest regarding the publication of this paper.

LITERATURE CITED

Ailliot, P., D. Allard, V. Monbet, and P. Naveau, 2015 Stochastic weather generators: an overview of weather type models. Journal de la société française de statistique **156**: 101–113.

Guan, X., V. D. Nguyen, P. Voit, B. Merz, M. Heistermann, *et al.*, 2025 The ability of a stochastic regional weather generator to reproduce heavy-precipitation events across scales. Natural Hazards and Earth System Sciences **25**: 3075–3086.

Kilsby, C. G., P. Jones, A. Burton, A. Ford, H. J. Fowler, *et al.*, 2007 A daily weather generator for use in climate change studies. Environmental Modelling & Software **22**: 1705–1719.

Knutti, R., M. R. Allen, P. Friedlingstein, J. M. Gregory, G. C. Hegerl, *et al.*, 2008 A review of uncertainties in global temperature projections over the twenty-first century. Journal of Climate **21**: 2651–2663.

Najibi, N., A. J. Perez, W. Arnold, A. Schwarz, R. Maendly, *et al.*, 2024 A statewide, weather-regime based stochastic weather generator for process-based bottom-up climate risk assessments in california–part i: Model evaluation. Climate Services **34**: 100489.

Nandan, R., V. Bandaru, P. Meduri, C. Jones, and R. Lollato, 2024 Evaluating the utility of weather generators in crop simulation models for in-season yield forecasting. Agricultural Systems **220**: 104082.

Palmer, T., G. Shutts, R. Hagedorn, F. Doblas-Reyes, T. Jung, *et al.*, 2005 Representing model uncertainty in weather and climate prediction. Annu. Rev. Earth Planet. Sci. **33**: 163–193.

Palmer, T. N., 2000 Predicting uncertainty in forecasts of weather and climate. Reports on progress in Physics **63**: 71.

Schuol, J. and K. Abbaspour, 2007 Using monthly weather statistics to generate daily data in a swat model application to west africa. Ecological modelling **201**: 301–311.

Semenov, M. A., 2008 Simulation of extreme weather events by a stochastic weather generator. Climate Research **35**: 203–212.

Semenov, M. A., R. J. Brooks, E. M. Barrow, and C. W. Richardson, 1998 Comparison of the wgen and lars-wg stochastic weather generators for diverse climates. Climate research **10**: 95–107.

Wilks, D., 1999a Simultaneous stochastic simulation of daily precipitation, temperature and solar radiation at multiple sites in complex terrain. Agricultural and Forest Meteorology **96**: 85–101.

Wilks, D. S., 1998 Multisite generalization of a daily stochastic precipitation generation model. journal of Hydrology **210**: 178–191.

Wilks, D. S., 1999b Interannual variability and extreme-value characteristics of several stochastic daily precipitation models. Agricultural and forest meteorology **93**: 153–169.

Woodson, D., S. Gangopadhyay, L. Bearup, A. Verdin, E. Shamir, *et al.*, 2025 wxgenr: An r package for stochastic weather generation with seasonality. SoftwareX **31**: 102209.

Zippenfenig, P., 2023 Open-meteo.com weather api.

How to cite this article: Kılıç, N. H., and Sevin, A. Stochastic Weather Simulation of Türkiye's Geographical Regions: A Monte Carlo Framework. *ADBA Computer Science*, 3(1), 37-50, 2026.

Licensing Policy: The published articles in ACS are licensed under a Creative Commons Attribution-NonCommercial 4.0 International License.